

# An Assessment of the vdW-TS Method for Extended Systems

W. A. Al-Saidi,<sup>\*,†,‡</sup> Vamsee K. Voora,<sup>†</sup> and Kenneth D. Jordan<sup>\*,†</sup>

<sup>†</sup>Department of Chemistry and Center for Molecular and Materials Simulations, University of Pittsburgh, Pittsburgh, Pennsylvania 15260, United States

<sup>‡</sup>Department of Chemical and Petroleum Engineering, University of Pittsburgh, Pittsburgh, Pennsylvania 15261, United States

**ABSTRACT:** The Tkatchenko–Scheffler vdW-TS method [*Phys. Rev. Lett.* **2009**, *102*, 073005] has been implemented in a plane-wave DFT code and used to characterize several dispersion-dominated systems, including layered materials, noble-gas solids, and molecular crystals. Full optimizations of the structures, including relaxation of the stresses on the unit cells, were carried out. Internal geometrical parameters, lattice constants, bulk moduli, and cohesive energies are reported and compared to experimental results.

## 1. INTRODUCTION

The computational efficiency of density functional theory (DFT)<sup>1</sup> has made it the most widely used method for calculating the electronic structure of solids and their surfaces. However, a major drawback of local and semilocal density functionals in weakly interacting systems is the failure to describe long-range dispersion interactions.<sup>2</sup> This deficiency of commonly employed DFT methods precludes their use for quantitative prediction of lattice constants and cohesive energies of layered materials and molecular crystals.

The development of procedures for correcting DFT for dispersion is an active area of research. Among the most popular methods are the DFT-D2<sup>3</sup> and DFT-D3<sup>4</sup> procedures of Grimme and co-workers. In the DFT-D2 approach, dispersion corrections are introduced by adding damped atom–atom  $C_6/R^6$  terms, and in the DFT-D3 approach, they are introduced through damped atom–atom  $C_6/R^6$  and  $C_8/R^8$  terms. In the DFT-D2 method, the  $C_6$  coefficients are independent of the chemical environment. This deficiency is partially remedied in DFT-D3, where the  $C_6$  coefficients depend on the coordination number of the atoms. Closely related approaches include the DFT/CC procedure of Rubeš and co-workers,<sup>5,6</sup> the DFT-*lg* method of Liu and Goddard,<sup>7</sup> and the vdW-TS approach of Tkatchenko and Scheffler.<sup>8,9</sup> Of these approaches, vdW-TS is particularly intriguing because of how the  $C_6$  coefficients depend on the chemical environment. Specifically, the atomic polarizabilities used to calculate the  $C_6$  coefficients are scaled by the ratio of volumes of the atoms in the molecule or solid to those of free atoms. The atomic volumes are obtained using a Hirshfeld decomposition scheme<sup>10</sup> building on the work of Johnson and Becke.<sup>11,12</sup> The vdW-TS method employs a single universal functional-dependent damping parameter chosen by fitting to accurate coupled cluster singles plus doubles with perturbative triples [CCSD(T)]<sup>13</sup> interaction energies<sup>14</sup> for the S22 set of dimers.<sup>15</sup> In this study, we explore the utility of the vdW-TS procedure for describing several crystalline materials, including noble gas solids, molecular crystals, and layered materials, in which dispersion interactions are important. To this end, we have implemented the vdW-TS scheme in the Vienna *ab initio* simulation package (VASP) code.<sup>16,17</sup> To assess the performance of the method, we compare the calculated structures, cohesive energies, and bulk moduli with the corresponding experimental values when available. Cohesive

energies were calculated for the noble gas solids and the molecular crystals but not for the layered materials and the covalent solids. Comparison is also made with the results of DFT calculations with the Perdew–Becke–Ernzerhof (PBE)<sup>18</sup> functional and with the DFT-D2<sup>3</sup> method used in conjunction with the PBE functional, reporting the results of ref 19 when available and carrying out the required calculations in the other cases.

## 2. COMPUTATIONAL DETAILS

The vdW-TS scheme was originally implemented in FHI-aims code which uses numerical atomic basis sets.<sup>20</sup> In the present study, we have implemented the vdW-TS<sup>8</sup> method in the VASP code,<sup>16,17</sup> which employs plane-wave basis sets. Our implementation is general, allowing for optimization of both the atomic coordinates and the lattice parameters of periodic systems. The vdW-TS scheme can be employed with a wide range of functionals, but the present study focuses on its use with the PBE functional, with the PBE + vdW-TS procedure being denoted PBE-TS for short. Limited results will also be presented for use of the vdW-TS procedure in conjunction with the PBEsol<sup>21</sup> functional, with the resulting procedure being denoted PBEsol-TS.

The calculations were performed using projected augmented waves (PAW) with standard PAW data sets.<sup>22,23</sup> In the SCF cycles, a convergence criterion of  $10^{-6}$  eV on the energies was used. Structural parameters were optimized using an optimization threshold of 1 meV/Å for the forces on each atom. Details on the plane-wave cutoffs and *k*-point grids used in the calculations are provided in Table 1. Here, we note that care was taken to ensure that the lattice constants and total energies are well converged with respect to the plane-wave cutoffs and *k*-point grids. The cohesive energies  $\Delta E_{\text{coh}}$  were computed using

$$\Delta E_{\text{coh}} = \frac{1}{n} E_{\text{solid}} - E_{\text{monomer}} \quad (1)$$

where the energy of the isolated system ( $E_{\text{monomer}}$ ) is obtained using a cubic supercell with a side length of 15 Å and *n* denotes the number of monomers per unit cell. In our sign convention, negative values of  $\Delta E_{\text{coh}}$  indicate stable systems.

**Received:** September 3, 2011

**Published:** February 24, 2012



**Table 1.** *k*-Point Grids and Plane-Wave Cutoffs Employed in the Calculations

| solid system                                | <i>k</i> -points <sup>a</sup> | plane-wave cutoff (eV) |
|---|-------------------------------|------------------------|
| noble gas solids                            | 8 × 8 × 8                     | 1000                   |
| α-nitrogen, CO <sub>2</sub> , and acetylene | 8 × 8 × 8                     | 1000                   |
| cubane                                      | 3 × 3 × 3                     | 1000                   |
| benzene, anthracene                         | 2 × 2 × 2                     | 800                    |
| naphthalene                                 | 2 × 2 × 2                     | 1000                   |
| cytosine                                    | 1 × 1 × 3                     | 800                    |
| graphite                                    | 16 × 16 × 8                   | 1000                   |
| <i>h</i> -BN                                | 16 × 16 × 8                   | 1500                   |
| V <sub>2</sub> O <sub>5</sub>               | 4 × 4 × 8                     | 1500                   |
| diamond and silicon                         | 16 × 16 × 16                  | 500                    |

<sup>a</sup>All grids are  $\Gamma$ -point-centered.

**2.1. The vdW-TS Scheme.** The vdW-TS method corrects for long-range dispersion interactions by adding a correction of the form

$$E_{\text{disp}} = -\frac{1}{2} \sum_{A,B} \frac{C_{6AB}}{r_{AB}^6} f_{\text{damp}}(r_{AB}) \quad (2)$$

to the DFT energy. The sum is over all atomic pairs A and B including the images obtained by lattice translations.  $r_{AB}$  is the distance between atoms A and B, and  $f_{\text{damp}}(r_{AB})$  is a damping function that prevents divergence at short distances and double counting of short-range dispersion contributions. In our implementation of the method, we used a straightforward summation over images until the dispersion energy converges to a specified tolerance. The results reported were obtained with a tolerance of  $10^{-4}$  eV on the sum. Test calculations with a  $10^{-5}$  eV tolerance did not result in significant changes in the lattice constants. Although it would be preferable to use an Ewald-type procedure to sum the dispersion contributions as discussed in refs 24 and 25, the direct approach is adequate for the current purposes.

The  $C_6$  coefficients in the vdW-TS scheme depend on the chemical environment by exploiting the relationship between the polarizability and volume.<sup>26</sup> Specifically, for interactions between two chemically equivalent A atoms, Tkatchenko and Scheffler define the effective  $C_6$  coefficient as

$$C_{6AA}^{\text{eff}} = \left( \frac{V_A^{\text{eff}}}{V_A^{\text{free}}} \right)^2 C_{6AA}^{\text{free}} \quad (3)$$

where  $V_A^{\text{free}}$  and  $V_A^{\text{eff}}$  are the Hirshfeld volumes of atom A in isolation and in the bonding environment, respectively.  $C_{6AA}^{\text{free}}$  is the homonuclear  $C_6$  coefficient from the compilation of Chu and Dalgarno<sup>27</sup> where the values were obtained using a self-interaction free linear response time-dependent DFT approach. The effective dispersion coefficients  $C_{6AA}^{\text{free}}$  between chemically inequivalent atoms A and B are calculated using the combination rule

$$C_{6AB}^{\text{eff}} = \frac{2C_{6AA}^{\text{eff}}C_{6BB}^{\text{eff}}}{\frac{\alpha_B}{\alpha_A}C_{6AA}^{\text{eff}} + \frac{\alpha_A}{\alpha_B}C_{6BB}^{\text{eff}}} \quad (4)$$

The atomic polarizabilities in this expression are defined as

$$\alpha_A = \frac{V_A^{\text{eff}}}{V_A^{\text{free}}} \alpha_A^{\text{free}} \quad (5)$$

where  $\alpha_A^{\text{free}}$  is the static isotropic polarizability for the free atom A obtained from the database of Chu and Dalgarno.<sup>27</sup> The damping function used in the TS scheme is

$$f_{\text{damp}}(R_{AB}, R_{AB}^{\text{eff}}) = \frac{1}{1 + \exp\left(-d\left(\frac{R_{AB}}{s_r R_{AB}^{\text{eff}}} - 1\right)\right)} \quad (6)$$

When using the vdW-TS scheme in conjunction with the PBE functional, we adopt the same values for the parameters  $d$  and  $s_r$  as used in the work of Tkatchenko and Scheffler (i.e.,  $d = 20.0$  and  $s_r = 0.94$ ).<sup>8</sup>  $R_{AB}^{\text{eff}}$  is the sum of effective van der Waals radii of atoms A and B atoms in the molecule (or crystal). The effective van der Waals radius of atom A is given by

$$R_A^{\text{eff}} = \left( \frac{V_A^{\text{eff}}}{V_A^{\text{free}}} \right)^{1/3} R_A^{\text{free}} \quad (7)$$

where  $R_A^{\text{free}}$  is defined as the radius at which the electron density of the free atom is the same as that of the noble gas atom (from the same row of the periodic table) at its van der Waals radius. The  $R_A^{\text{free}}$  values for the noble gases were taken from the compilation of Bondi.<sup>28</sup>

As noted above, we have also parametrized the vdW-TS correction for use with the PBEsol functional, which was designed to describe condensed phase systems.<sup>21</sup> This was accomplished by fitting the PBEsol-TS interaction energies to the CCSD(T) results for the S22 dimer set.<sup>14</sup> The PBEsol-TS calculations on the dimers were performed using the FHI-aims package<sup>20</sup> with the tier-3 basis set. This gave a value of 1.06 for  $s_r$  compared to the 0.94 value used in the PBE-TS procedure.

### 3. RESULTS AND DISCUSSION

**3.1. Noble Gas Solids.** The Ne, Ar, Kr, and Xe crystals adopt a face-centered cubic [FCC] structure. Table 2 reports the lattice parameters, bulk moduli, and cohesive energies of these crystals obtained from the PBE-TS procedure as well as from previous PBE,<sup>19</sup> PBE-D2,<sup>19</sup> RPA/ACFDT,<sup>29</sup> and vdW-DF<sup>30</sup> calculations and from experimental measurements.<sup>31–38</sup> The RPA/ACFDT approach refers to the random phase approximation within the adiabatic connection fluctuation-dissipation theorem scheme.<sup>39</sup> The vdW-DF method recovers dispersion effects by using a nonlocal correlation functional.<sup>40</sup>

Table 2 also reports the results of Rościszewski et al.<sup>41</sup> obtained using the incremental method (IM),<sup>42</sup> which gives near complete-basis-set limit CCSD(T)<sup>13</sup> quality interaction energies. IM results are reported for 2-body interactions only [IM(2B)] and for 2+3+4-body interactions without [IM-(2+3+4B)] and with [IM(2+3+4B+ZPE)] vibrational zero-point energy corrections.

The theoretical results reported for the inert gas crystals in the present study and in refs 19, 29, and 30 neglect vibrational zero-point corrections. The situation concerning many-body effects is more complicated because local and semilocal DFT include short-range many-body contributions. Nonetheless, the dominant many-body contributions for the inert gas systems, and for several of the other systems considered in this paper, should arise from long-range dispersion interactions which are not recovered by the PBE or other GGA functionals. Thus, we believe it is most meaningful to compare the results of the DFT calculations to those from the incremental method with 2-body contributions.

**Table 2.** Lattice Constants, Bulk Modulus, and Cohesive Energies of Noble Gas Crystals

|                               | Ne                 | Ar                 | Kr                 | Xe                 |
|-------------------------------|--------------------|--------------------|--------------------|--------------------|
| <i>a</i> (Å)                  |                    |                    |                    |                    |
| exptl                         | 4.464 <sup>a</sup> | 5.300 <sup>b</sup> | 5.646 <sup>c</sup> | 6.132 <sup>d</sup> |
| IM(2 + 3+4B+ZPE) <sup>e</sup> | 4.468              | 5.311              | 5.633              | 6.111              |
| IM(2 + 3+4B) <sup>e</sup>     | 4.297              | 5.251              | 5.598              | 6.087              |
| IM(2B) <sup>e</sup>           | 4.277              | 5.213              | 5.556              | 6.054              |
| PBE <sup>f</sup>              | 4.56               | 5.92               | 6.49               | 7.01               |
| PBE-D2 <sup>f</sup>           | 4.23               | 5.38               | 5.64               | 6.06               |
| PBE-TS                        | 4.42               | 5.51               | 5.90               | 6.37               |
| RPA <sup>g</sup>              | 4.5                | 5.3                | 5.7                |                    |
| vdW-DF <sup>h</sup>           | 4.56               | 6.00               |                    |                    |
| $\Delta E_{coh}$ (meV/atom)   |                    |                    |                    |                    |
| exptl                         | -20 <sup>i</sup>   | -80 <sup>j</sup>   | -116 <sup>j</sup>  | -165 <sup>j</sup>  |
| IM(2 + 3+4B+ZPE) <sup>e</sup> | -20                | -80                | 116                | 165                |
| IM(2 + 3+4B) <sup>e</sup>     | -26                | -88                | -122               | -170               |
| IM(2B) <sup>e</sup>           | -27                | -94                | -132               | -185               |
| PBE <sup>f</sup>              | -20                | -22                | -25                | -28                |
| PBE-D2 <sup>f</sup>           | -58                | -88                | -145               | -218               |
| PBE-TS                        | -43                | -83                | -97                | -117               |
| RPA <sup>g</sup>              | -17                | -83                | -112               |                    |
| $B_0$ (GPa)                   |                    |                    |                    |                    |
| exptl                         | 1.1 <sup>a</sup>   | 2.7 <sup>b</sup>   | 3.6 <sup>k</sup>   | 3.6 <sup>l</sup>   |
| IM(2 + 3+4B+ZPE) <sup>e</sup> | 1.1                | 2.8                | 3.3                | 3.7                |
| IM(2 + 3+4B) <sup>e</sup>     | 1.9                | 3.3                | 3.6                | 4.0                |
| IM(2B) <sup>e</sup>           | 2.0                | 3.8                | 4.1                | 4.6                |
| PBE <sup>f</sup>              | 1                  | <1                 | <1                 | <1                 |
| PBE-D2 <sup>f</sup>           | 4                  | 3                  | 4                  | 6                  |
| PBE-TS                        | 2.62               | 2.72               | 2.58               | 2.35               |
| vdW-DF <sup>h</sup>           | 2.1                | 0.9                |                    |                    |

<sup>a</sup>ref 35. <sup>b</sup>ref 36. <sup>c</sup>ref 37. <sup>d</sup>ref 38. <sup>e</sup>ref 41. <sup>f</sup>ref 19. <sup>g</sup>ref 29. <sup>h</sup>ref 30. <sup>i</sup>ref 32. <sup>j</sup>ref 31. <sup>k</sup>ref 34. <sup>l</sup>ref 33.

In analyzing the trends along the sequence of inert gas crystals it is useful to first consider the vibrational zero-point and many-body corrections reported by Rościszewski et al. As expected, the zero-point correction to the lattice constants falls off as one progresses from Ne (0.17 Å) to Xe (0.02 Å). In contrast, the 3+4-body corrections to the lattice constants are more nearly constant, ranging from 0.02 Å to 0.04 Å. Both zero-point energy and many-body contributions lead to a decrease in the values of the bulk moduli, with the combination of these two effects causing nearly a factor of 2 change in the bulk modulus of crystalline Ne and 20–22% decreases in the bulk moduli of the other rare gas solids. The zero-point contributions to the cohesive energies are roughly constant in an absolute sense, ranging from 5 to 8 meV/atom for the various inert gas solids, while the many-body correction to the cohesive energy grows from 1 meV/atom for Ne to 15 meV/atom for crystalline Xe.

As expected, PBE calculations without dispersion corrections considerably overestimate the lattice constants and underestimate the cohesive energies and bulk moduli of crystalline Ar, Kr, and Xe. Inclusion of 2-body dispersion interactions through either the PBE-D2 or PBE-TS procedures greatly improves agreement with experimental results for these solids. However, in assessing the performance of these methods, it is most meaningful, as mentioned above, to compare with the IM(2B) results.

As seen from Table 2, the values of the lattice constants predicted by PBE-D2 are in better agreement with the IM(2B)

predictions than are those calculated using PBE-TS, which overestimates the IM(2B) values of the lattice constants by a few tenths of an Ångstrom. For the Ar crystal, both the PBE-D2 and PBE-TS methods give values of the cohesive energy close to the IM(2B) result. However, using the IM(2B) results as the reference, for the Kr and Xe crystals the PBE-TS method underestimates in magnitude the cohesive energies by 26 and 37%, respectively, while the PBE-D2 method overestimates in magnitude the cohesive energies by 10–20%. Roughly speaking, the trends in calculated values of the bulk moduli track those in the cohesive energies. Namely, for Ar, both the PBE-TS and PBE-D2 methods give a value of the bulk modulus close to the experimental value, whereas for Kr and Xe, the PBE-TS method underestimates and the PBE-D2 method overestimates the values of the bulk modulus.

RPA/ACFDT values of the lattice constants and cohesive energies of the Ne, Ar, and Kr crystals, reported by Harl and Kresse,<sup>29</sup> are in reasonable agreement with the IM(2+3+4B) values. Specifically, with regard to the cohesive energies, the RPA values of crystalline Ar and Kr are within 8% of the IM(2+3+4B) values while for crystalline Ne, the RPA result is about 35% too small in magnitude.

vdW-DF values for lattice constants and bulk moduli of crystalline Ne and Ar have been reported in ref 30. Surprisingly, the values of the lattice constants from the vdW-DF calculations are nearly the same as those from PBE calculations without dispersion corrections. Also, while the vdW-DF value of the bulk modulus of crystalline Ne is in excellent agreement with the IM(2B) result, for the Ar crystal the vdW-DF method gives a value of the bulk modulus much smaller than the IM(2B) result.

In contrast to the situation for crystalline Ar, Kr, and Xe, for crystalline Ne the PBE calculations without dispersion corrections give values of the cohesive energy, lattice constant, and bulk modulus in close agreement with experimental results. As a consequence, when dispersion corrections are included, the Ne crystal is predicted to be significantly overbound and the bulk modulus to be considerably overestimated. The apparent good agreement between PBE and the experimental values of the cohesive energy, lattice constants, and bulk modulus for crystalline Ne is fortuitous, being largely due to the neglect of vibrational zero-point effects in the calculations.

For understanding the trends in the solids, it is instructive to examine the equilibrium bond lengths ( $R_e$ ) and dissociation energies ( $D_e$ ) for the inert gas dimers reported in Table 3. For  $\text{Ne}_2$ , the PBE functional without dispersion corrections gives a binding energy about a factor of two too large in magnitude compared to the CCSD(T)<sup>43</sup> and experimental values.<sup>44</sup> On the other hand, for the heavier inert gas dimers, the PBE functional gives binding energies of one-quarter to nearly one-half of the experimental values, with the result that the dispersion-corrected DFT calculations fare better for these species. For  $\text{Ar}_2$ ,  $\text{Kr}_2$ , and  $\text{Xe}_2$ , the PBE-D2 method gives bond lengths closer to experimental values than does the PBE-TS method, while the PBE-TS method gives binding energies closer to the experimental values than does the PBE-D2 method.

Table 3 also reports experimentally deduced values of the  $C_6$  coefficients for the inert gas dimers as well as the values of the  $C_6$  coefficients used in the PBE-D2 and PBE-TS calculations. The  $C_6$  coefficients for the inert gas dimers are significantly overestimated in the PBE-D2 procedure, while the  $C_6$  coefficients in the PBE-TS scheme are very close to those

**Table 3.**  $C_6$  Coefficients, Bond Lengths, and Bond Energies of Noble Gas Dimers

|                                    | Ne     | Ar      | Kr      | Xe      |
|------------------------------------|--------|---------|---------|---------|
| $C_6$ (Hartree/Bohr <sup>6</sup> ) |        |         |         |         |
| expt <sup>a</sup>                  | 6      | 64      | 130     | 286     |
| PBE-D2                             | 11     | 80      | 208     | 521     |
| PBE-TS                             | 6      | 64      | 130     | 286     |
| $l$ (Å)                            |        |         |         |         |
| expt <sup>b</sup>                  | 3.091  | 3.7565  | 4.008   | 4.3627  |
| CCSD(T) <sup>c</sup>               | 3.105  | 3.793   | 4.065   | 4.409   |
| PBE                                | 3.102  | 4.120   | 4.307   | 4.596   |
| PBE-D2                             | 2.881  | 3.733   | 3.991   | 4.339   |
| PBE-TS                             | 3.081  | 3.836   | 4.141   | 4.582   |
| $D_e$ (meV)                        |        |         |         |         |
| expt <sup>b</sup>                  | -3.638 | -12.333 | -17.326 | -24.309 |
| CCSD(T) <sup>c</sup>               | -3.47  | -11.32  | -15.81  | -22.91  |
| PBE                                | -5.55  | -5.86   | -6.61   | -6.60   |
| PBE-D2                             | -12.40 | -16.83  | -25.37  | -35.34  |
| PBE-TS                             | -9.03  | -15.55  | -18.19  | -21.13  |

<sup>a</sup>ref 45. <sup>b</sup>ref 44. <sup>c</sup>ref 43.

calculated by Kumar and Meath<sup>45</sup> using experimental data. Since the  $R^{-8}$  and  $R^{-10}$  dispersion terms make significant contributions to the dimer binding energies, particularly for the heavier inert gas atoms, one could justify the use of somewhat enhanced values of the  $C_6$  coefficients as a means of including in an effective manner the  $R^{-8}$  and  $R^{-10}$  dispersion contributions. Notwithstanding, it appears that the large values of the  $C_6$  coefficients in the PBE-D2 method contribute to the overestimation of the magnitude of the dissociation energies. Obviously, it would be preferable to explicitly account for the  $R^{-8}$  and  $R^{-10}$  dispersion contributions.

The fact that the PBE functional gives attractive interactions between inert gas atoms is generally viewed as an artifact, resulting primarily from deficiencies in the exchange functional.<sup>46,47</sup> However, it should also be kept in mind that the PBE functional does recover short-range interatomic correlation.<sup>2,48</sup> Thus, it is not clear that the binding of inert gas dimers in calculations using the PBE functional is purely an artifact.

**3.2. Molecular Crystals.** **3.2.1.  $\alpha$ -Nitrogen,  $\text{CO}_2$ , Acetylene, and Cubane.** At low temperatures,  $\alpha$ -nitrogen and carbon dioxide crystallize in cubic structures with  $\text{Pa}3$  (Figure 1) space group symmetry with four molecules per unit cell. For acetylene, the stable phase at  $T = 0$  K is orthorhombic, while at  $T = 133\text{--}191$  K, the stable phase is  $\text{Pa}3$ . In the present calculations, the  $\text{Pa}3$  space group was employed for all three of these crystals. The arrangement of the molecules in the  $\text{Pa}3$  crystal of acetylene is shown in Figure 1. In the cubane crystal, the molecules have an  $\text{R}\bar{3}$  rhombohedral arrangement, as illustrated in Figure 2.

Table 4 summarizes the lattice parameters, cohesive energies, bulk moduli, and internal bond lengths of the crystals of  $\alpha$ -nitrogen,  $\text{CO}_2$ , and acetylene. As expected, the inclusion of dispersion corrections has almost no effect on the values of the internal bond lengths, which are already well described by the dispersion-uncorrected PBE functional. The polarizabilities of  $\text{N}_2$ ,  $\text{CO}_2$ , and  $\text{C}_2\text{H}_2$  are roughly comparable to that of the Ar atom. Hence, as for the Ar crystal, many-body effects are not expected to play a major role in determining the structures and lattice constants of these crystals. In fact, a recent study reports a 3-body dispersion contribution of only 1.2 kJ/mol<sup>49</sup> to the cohesive energy of crystalline  $\text{CO}_2$ , compared to the

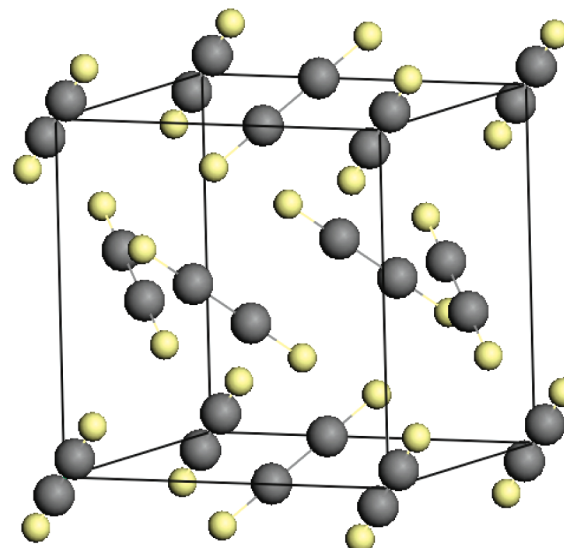


**Figure 1.** Acetylene crystal with  $\text{Pa}3$  space group structure.

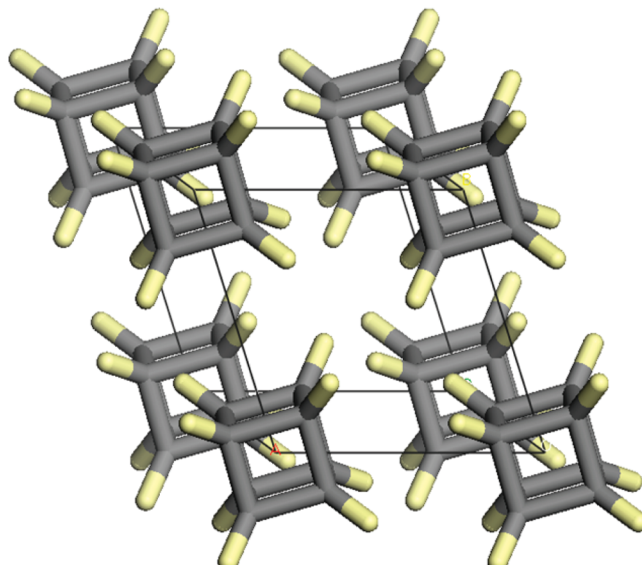


**Figure 2.** Crystal structure of cubane with  $\text{R}\bar{3}$  symmetry.

experimental value of -27 kJ/mol<sup>50</sup> for the net cohesive energy. The experimental value of the cohesive energy of the nitrogen crystal reported in Table 4 has been corrected for the zero-point vibrational energy ( $\sim 1.4$  kJ/mol). LeSar and Gordan<sup>51</sup> have estimated that the vibrational zero-point correction to the cohesive energy of crystalline  $\text{CO}_2$  is 2.5 kJ/mol, and the vibrational zero-point correction for the crystalline acetylene is expected to be comparable in magnitude.

For the low temperature  $\alpha$ -phase of nitrogen, the experimental value of the lattice parameter is 5.649 Å at  $T = 20$  K.<sup>52</sup> The PBE calculations overestimate the lattice constant, giving a value of 6.19 Å, and underestimate the cohesive energy, giving a value of 2.6 kJ/mol compared to the experimental<sup>53</sup> value of 7.6 kJ/mol (including the zero-point correction). The PBE-TS and PBE-D2 calculations both give a lattice parameter of 5.65 Å, in agreement with the experimental value, and give values of the cohesive energy in reasonable agreement with the experimental values, albeit overestimated in magnitude (by 0.9 and 1.8 kJ/mol with PBE-TS and PBE-D2,

**Table 4.** Lattice Parameters, Internal Bond Lengths, Cohesive Energies, and Bulk Moduli for N<sub>2</sub>, CO<sub>2</sub>, and C<sub>2</sub>H<sub>2</sub> Crystals with *Pa*3 Symmetry

|                             | N <sub>2</sub>          | CO <sub>2</sub>         | C <sub>2</sub> H <sub>2</sub> |
|-----------------------------|-------------------------|-------------------------|-------------------------------|
| <i>a</i> (Å)                |                         |                         |                               |
| exptl                       | 5.649 <sup>a</sup>      | 5.624 <sup>b</sup>      | 6.094 <sup>c</sup>            |
| PBE <sup>d</sup>            | 6.19                    | 6.02                    | 6.36                          |
| PBE-D2 <sup>d</sup>         | 5.65                    | 5.65                    | 5.79                          |
| PBE-TS                      | 5.65                    | 5.79                    | 5.97                          |
| $\Delta E_{coh}$ (kJ/mol)   |                         |                         |                               |
| exptl                       | -7.6 <sup>e</sup>       | -27.2 <sup>f</sup>      | -25.2 <sup>f</sup>            |
| PBE <sup>d</sup>            | -2.6                    | -10.3                   | -12.1                         |
| PBE-D2 <sup>d</sup>         | -8.5                    | -24.3                   | -27.1                         |
| PBE-TS                      | -9.4                    | -25.2                   | -27.0                         |
| <i>B</i> <sub>0</sub> (GPa) |                         |                         |                               |
| exptl                       | 6 <sup>g</sup>          |                         |                               |
| PBE <sup>d</sup>            | <1                      | 2.60                    | 2.22                          |
| PBE-D2 <sup>d</sup>         | 2                       | 7.70                    | 6.00                          |
| PBE-TS                      | 2.99                    | 7.28                    | 6.27                          |
| internal bond lengths (Å)   |                         |                         |                               |
|                             | <i>r</i> <sub>N-N</sub> | <i>r</i> <sub>C-O</sub> | <i>r</i> <sub>C-H</sub>       |
| exptl                       | 1.066 <sup>a</sup>      | 1.155 <sup>b</sup>      |                               |
| PBE <sup>d</sup>            | 1.112                   | 1.175                   | 1.072                         |
| PBE-D2 <sup>d</sup>         | 1.112                   | 1.174                   | 1.073                         |
| PBE-TS                      | 1.112                   | 1.174                   | 1.072                         |

<sup>a</sup>ref 52. <sup>b</sup>ref 71. <sup>c</sup>ref 72. <sup>d</sup>ref 19. <sup>e</sup>ref 53. <sup>f</sup>ref 50. <sup>g</sup>ref 73.

respectively). However, it should be kept in mind that the experimental result includes the effect of many-body dispersion, which could contribute on the order of 1 kJ/mol and which is not accounted for in the calculated values.

We were unable to locate an experimental value of the bulk modulus of the  $\alpha$ -phase of nitrogen, but note that the PBE-D2 and PBE-TS approaches give values of the bulk modulus 2 to 3 times greater than that obtained from the PBE calculations. Similar trends are found for the CO<sub>2</sub> and acetylene crystals, with significant improvements being found in the calculated lattice constants, cohesive energies, and bulk moduli upon inclusion of dispersion corrections by either the PBE-TS or PBE-D2 methods.

The trends in the calculated results for the cubane crystal are reported in Table 5 and are consistent with those for the N<sub>2</sub>,

**Table 5.** Lattice Parameters, Cohesive Energies, Bulk Moduli, and Internal Bond Lengths for the Cubane Crystal

|                     | <i>a</i> (Å)      | $\alpha$ (deg)       | $\Delta E_{coh}$ (kJ/mol) | <i>B</i> <sub>0</sub> (GPa) |
|---------------------|-------------------|----------------------|---------------------------|-----------------------------|
| exptl               | 5.20 <sup>a</sup> | 72.7(1) <sup>a</sup> | -80.08 <sup>b</sup>       |                             |
| PBE                 | 5.83              | 71.35                | -6.68                     | 1.0                         |
| PBE-D2              | 5.01              | 72.34                | -79.06                    | 15.1                        |
| PBE-TS              | 5.26              | 72.25                | -90.39                    | 12.1                        |
| vdW-DF <sup>c</sup> | 5.45              | 73.0                 | 74.29                     | 7.2                         |

<sup>a</sup>ref 74. <sup>b</sup>ref 54. <sup>c</sup>ref 55.

CO<sub>2</sub>, and acetylene crystals discussed above, namely, that the PBE functional considerably overestimates the *a* lattice constant and drastically underestimates the magnitudes of the cohesive energies and bulk modulus. Both the PBE-D2 and PBE-TS procedures perform much better, although the PBE-D2 approach overestimates the lattice constant by 0.2 Å and the PBE-TS method gives a cohesive energy about 10 kJ/mol larger in magnitude than the experimental value.<sup>54</sup> Much of the

discrepancy between the PBE-TS and measured values of the cohesive energy is expected to be due to the combination of the vibrational ZPE, finite temperature, and many-body effects, all of which impact the experimental value.

vdW-DF calculations have been reported for the cubane crystal.<sup>55</sup> While the properties obtained with this approach are in better agreement with experimental results than those calculated with the PBE functional, it performs somewhat more poorly than either the PBE-TS or PBE-D2 methods in predicting the values of the *a* lattice constant and the cohesive energy.

**3.2.2. Aromatic Systems.** The benzene, naphthalene, anthracene, and cytosine crystals were chosen to test the PBE-TS method in systems where  $\pi-\pi$  interactions are important. Cytosine is of interest because of its participation in a Watson-Crick base pair.

**3.2.2.1. Benzene.** Experimentally, benzene has an orthorhombic crystal structure with the *Pbca* space group with lattice parameters of *a* = 7.355, *b* = 9.371, and *c* = 6.700 Å.<sup>56</sup> (These results are from high resolution powder diffraction measurements at *T* = 4.2 K.) The arrangement of the molecules in the crystal is shown in Figure 3. The calculated values of the lattice parameters, cohesive energies, and bulk modulus are reported in Table 6.

The *a*, *b*, and *c* lattice parameters of the benzene crystal are all significantly overestimated with the PBE functional. Both the PBE-D2 and PBE-TS approaches lead to lattice parameters in much closer agreement with the experimental results, with the PBE-TS functional performing better in this context. The PBE-TS, PBE-D2, and experimental<sup>50</sup> values of the cohesive energies for the benzene crystal are -65.1, -55.2, and -44.6 kJ/mol, respectively.<sup>50</sup> The experimental value of the cohesive energy was obtained from the measured heat of sublimation, and the finite temperature plus zero-point vibrational energy contributions to this result have been estimated to be ~7 kJ/mol.<sup>57</sup> In addition, 3-body dispersion interactions have been estimated to contribute about 6.5 kJ/mol to the cohesive energy of the benzene crystal.<sup>58</sup> Thus, the corrected 2-body cohesive energy of benzene to which the comparison of the PBE-TS and PBE-D2 results should be made is about -58 kJ/mol. Both the PBE-D2 and PBE-TS methods do reasonably well at predicting the 2-body contribution of the cohesive energy of the benzene crystal. The calculations with the PBE functional underestimate the bulk modulus of the benzene crystal by about a factor of 8. Both dispersion-corrected methods lead to values of the bulk modulus in reasonable agreement with experimental values, with the PBE-D2 approach faring better.

Galli and co-workers<sup>57</sup> have calculated the cohesive energy and the bulk modulus of the benzene crystal using the RPA/ACDFT method. The resulting cohesive energy and bulk modulus are in good agreement with experimental results (after allowing for the ZPE and finite temperature contributions to the former).

**3.2.2.2. Naphthalene and Anthracene.** Both naphthalene and anthracene adopt a herringbone arrangement of the molecules in the crystal, as shown in Figure 3. As expected, the calculations with the PBE functional overestimate all three lattice constants of these crystals, with the errors being greatest for the *a* lattice constant. The calculations with the PBE functional underestimate the magnitudes of the cohesive energies of the naphthalene and anthracene crystals by factors of roughly five and nine, respectively. The calculated lattice

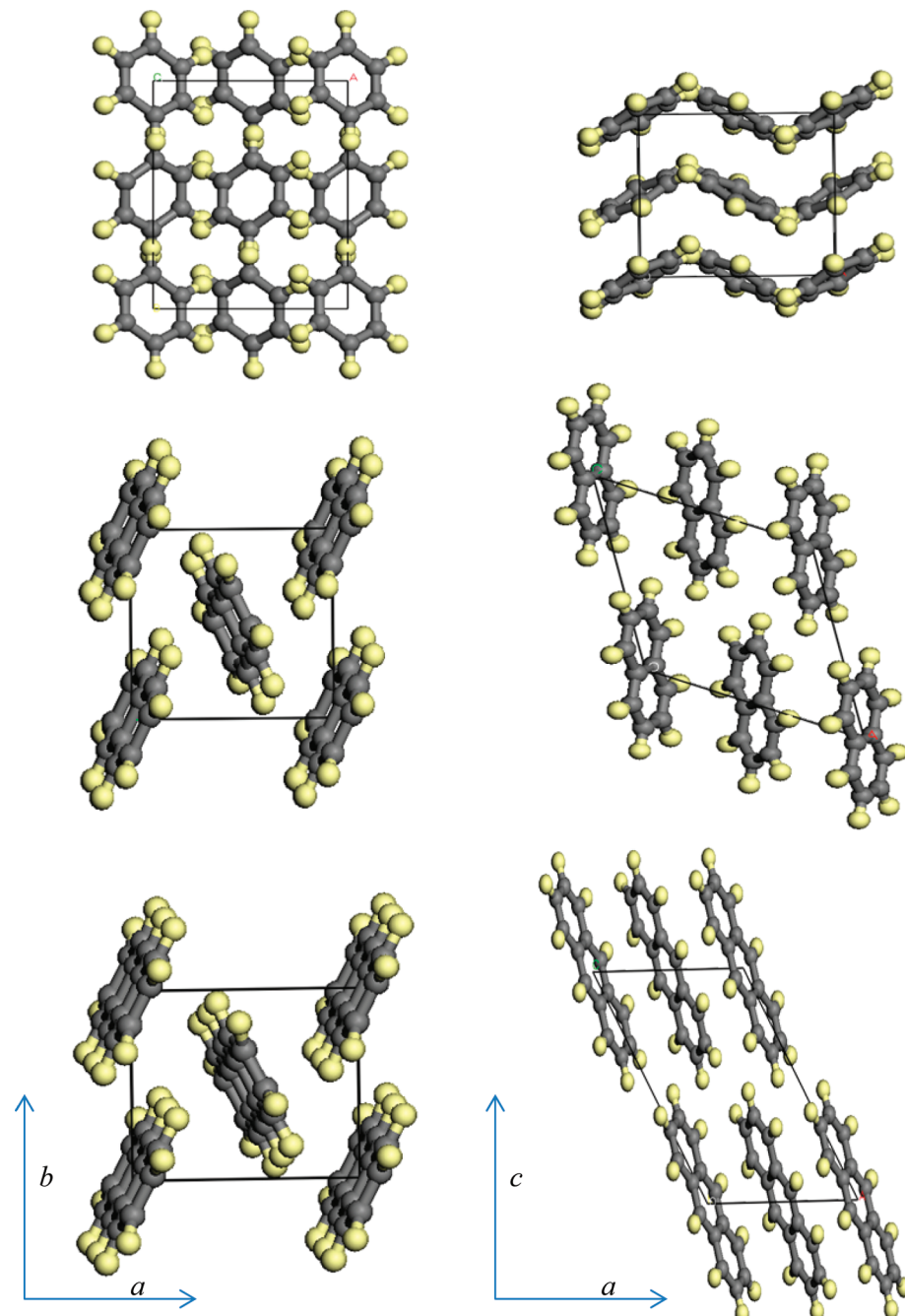


**Figure 3.** Crystal structures of benzene (top), naphthalene (middle), and anthracene (bottom) projected along the *ab* (left) and *ac* (right) planes. The benzene crystal has *Pbca* space group symmetry, and the naphthalene and anthracene crystals belong to the *P21/a* space group.

constants and cohesive energies are much closer to the experimental values when dispersion corrections are included. Recently, Fedorov et al.<sup>59</sup> applied the PBE-D2 method to the naphthalene and anthracene crystals, obtaining lattice constants slightly closer to the experimental values than those obtained in our PBE-D2 calculations. This is a consequence of these authors using larger van der Waals radii than used in our calculations.

We anticipate that vibrational zero-point energy and thermal corrections are of comparable importance for the cohesive energies of crystalline naphthalene and anthracene as for crystalline benzene, i.e., ~7 kJ/mol. In addition, we anticipate the 3-body dispersion contributions in crystalline naphthalene and anthracene to be about 12% of the 2-body dispersion

contribution calculated using the PBE-TS procedure, but of opposite sign, as found for the benzene crystal (i.e., to be on the order of 10 and 14 kJ/mol for the naphthalene and anthracene, respectively). Thus, it appears that, for the naphthalene and anthracene crystals, the PBE-TS method gives 2-body cohesive energies very close to the experimental values (sublimation energies) corrected for vibrational zero-point effects, finite temperature effects, and 3-body contributions, while the PBE-D2 method slightly underestimates the magnitude of the 2-body cohesive energies. We were unable to locate an experimental value of the bulk modulus of naphthalene. In the case of anthracene, the PBE method underestimates the bulk modulus by about a factor of 3.5, while the PBE-D2 and

**Table 6.** Lattice Constants, Cohesive Energies, and Bulk Moduli for Benzene, Naphthalene, and Anthracene Crystals

|                           | benzene                    |                      |                    | naphthalene        |                      |                    | anthracene          |                    |                     |
|---------------------------|----------------------------|----------------------|--------------------|--------------------|----------------------|--------------------|---------------------|--------------------|---------------------|
|                           | <i>a</i>                   | <i>b</i>             | <i>c</i>           | <i>a</i>           | <i>b</i>             | <i>c</i>           | <i>a</i>            | <i>b</i>           | <i>c</i>            |
| lattice constants (Å)     |                            |                      |                    |                    |                      |                    |                     |                    |                     |
| exptl                     | 7.355 <sup>a</sup>         | 9.371 <sup>a</sup>   | 6.700 <sup>a</sup> | 8.108 <sup>b</sup> | 5.940 <sup>b</sup>   | 8.647 <sup>b</sup> | 8.443 <sup>c</sup>  | 6.002 <sup>c</sup> | 11.124 <sup>c</sup> |
| PBE                       | 8.05 <sup>d</sup>          | 10.15 <sup>d</sup>   | 7.53 <sup>d</sup>  | 9.15               | 6.41                 | 9.04               | 9.29                | 6.31               | 11.39               |
| PBE-D2                    | 7.09 <sup>d</sup>          | 9.07 <sup>d</sup>    | 6.54 <sup>d</sup>  | 7.81               | 5.85                 | 8.50               | 8.13                | 5.90               | 10.93               |
| PBE-TS                    | 7.38                       | 9.20                 | 6.80               | 8.01               | 5.90                 | 8.62               | 8.33                | 5.95               | 11.10               |
| $\Delta E_{coh}$ (kJ/mol) |                            |                      |                    |                    |                      |                    |                     |                    |                     |
| exptl <sup>e</sup>        | −44.6 (−58.1) <sup>f</sup> |                      |                    | −70.4              |                      |                    | −101.1              |                    |                     |
| PBE                       | −9.7 <sup>d</sup>          |                      |                    | −8.58 <sup>g</sup> |                      |                    | −10.48 <sup>g</sup> |                    |                     |
| PBE-D2                    | −55.7 <sup>d</sup>         |                      |                    | −74.80             |                      |                    | −104.30             |                    |                     |
| PBE-TS                    | −65.1                      |                      |                    | −95.5              |                      |                    | −130.5              |                    |                     |
| RPA <sup>h</sup>          | −47                        |                      |                    | −47.43             |                      |                    |                     |                    |                     |
| PBE-lg <sup>g</sup>       | −28.29                     |                      |                    |                    |                      |                    |                     |                    |                     |
| $B_0$ (GPa)               |                            |                      |                    |                    |                      |                    |                     |                    |                     |
| exptl                     | 8 <sup>i</sup>             | 6.4–6.7 <sup>j</sup> |                    |                    | 7.3–7.5 <sup>i</sup> |                    |                     |                    |                     |
| PBE                       | 1 <sup>d</sup>             | 1.3                  |                    |                    | 1.7                  |                    |                     |                    |                     |
| PBE-D2                    | 10 <sup>d</sup>            | 11.9                 |                    |                    | 10.8                 |                    |                     |                    |                     |
| PBE-TS                    | 7.5                        | 11.8                 |                    |                    | 12.9                 |                    |                     |                    |                     |
| RPA <sup>h</sup>          | 7.5                        |                      |                    |                    |                      |                    |                     |                    |                     |

<sup>a</sup>ref 56. <sup>b</sup>ref 75. <sup>c</sup>ref 76. <sup>d</sup>ref 19. <sup>e</sup>The cohesive energies were taken as the median of the sublimation energies reported at 298 K in ref 50. <sup>f</sup>Includes corrections for vibrational zero-point energy<sup>57</sup> and three-body effects.<sup>58</sup> <sup>g</sup>ref 7. <sup>h</sup>ref 57. <sup>i</sup>ref 77. <sup>j</sup>ref 78.

PBE-TS procedures overestimate it by about 50 and 70%, respectively.

**3.2.2.3. Cytosine.** The cytosine crystal has an orthorhombic structure belonging to the  $P2_12_12_1$  space group. The PBE, PBE-D2, and PBE-TS methods all give values of the *b* lattice constant close to experimental values (Table 7). However, with

**Table 7.** Lattice Constants, Cohesive Energy, and Bulk Modulus for the Cytosine Crystal

|                     | lattice constants (Å) |                    |                    | $\Delta E_{coh}$ (kJ/mol) | $B_0$ (GPa) |
|---------------------|-----------------------|--------------------|--------------------|---------------------------|-------------|
|                     | <i>a</i>              | <i>b</i>           | <i>c</i>           |                           |             |
| exptl               | 13.041 <sup>a</sup>   | 9.494 <sup>a</sup> | 3.815 <sup>a</sup> | −155 <sup>b</sup>         |             |
| PBE <sup>c</sup>    | 12.00                 | 9.50               | 5.32               | −105.9                    | 4           |
| PBE-D2 <sup>c</sup> | 12.93                 | 9.46               | 3.64               | −162.5                    | 14          |
| PBE-TS              | 12.98                 | 9.46               | 3.72               | −171.2                    | 18          |

<sup>a</sup>ref 79. <sup>b</sup>ref 80. <sup>c</sup>ref 19.

the PBE functional, the *c* lattice constant is overestimated by about 1.5 Å, and the *a* lattice constant is underestimated by about 1.0 Å compared to the experimental values. Both the PBE-D2 and PBE-TS methods fare much better at predicting the values of the *a* and *c* lattice constants, with the largest discrepancy from experimental values being only 0.15 Å. Both dispersion-corrected DFT methods also fare much better than the PBE functional at predicting cohesive energies of solid cytosine. Although the calculations with the PBE functional underestimate the cohesive energy of the cytosine crystal by about 49 kJ/mol in magnitude, the PBE-D2 and PBE-TS approaches overestimate it by 12 and 16 kJ/mol, respectively. Correcting the experimental cohesive energy for vibrational zero-point thermal effects and for many-body contributions would reduce the disagreement between calculated and experimental values of the cohesive energy. We were unable to locate an experimental value of the bulk modulus for the cytosine crystal. Consistent with the results for the other systems studied, the PBE-D2 and PBE-TS methods give much

larger (by 3.5–4.5 times) values for the bulk modulus than obtained with the uncorrected PBE functional.

**3.3. Layered Materials.** **3.3.1. Graphite.** Graphite has an A–B layered structure comprised of two-dimensional hexagonal sheets. The corners of one sheet are aligned with the centers of the next. The distance between the sheets is given by the *c* lattice constant. The calculated lattice parameters and bulk modulus of graphite are reported in Table 8. The experimental values of the lattice parameters are *a* = 2.462 and *c* = 6.707 Å,<sup>60</sup> and the experimental values bulk modulus is 34–42 GPa.<sup>60,61</sup> The in-plane lattice constant *a* is essentially unaffected by the inclusion of dispersion corrections, and the PBE, PBE-D2, and PBE-TS approaches all give a value of *a* close to the experimental value. On the other hand, the calculations with the PBE functional overestimate the *c* lattice constant by about 2.1 Å. The PBE-D2 and PBE-TS methods give values of the *c* lattice constant much closer (within 0.26 Å and 0.06 Å, respectively) to the experimental value. The PBE functional drastically underestimates the bulk modulus of graphite, yielding a value of 1 GPa as compared to experimental values of 34 and 42 GPa.<sup>60,61</sup> The PBE-D2 method gives a value of 38 GPa for the bulk modulus, which is in between the two experimental values, while the PBE-TS method overestimates the bulk modulus, giving a value of 56 GPa. The vdW-DF1 method,<sup>62</sup> on the other hand, does poorly for graphite, considerably overestimating the *c* lattice parameter (*c* = 7.52 Å) and underestimating the value of the bulk modulus ( $B_0$  = 12 GPa). The vdW-DF2 method<sup>63</sup> does significantly better, but the *c* lattice parameter is still overestimated by about 0.25 Å. Graphite was studied recently using the RPA/ACFDT method, which gives a value of *c* = 6.68 Å,<sup>64</sup> in excellent agreement with the experimental value.

**3.3.2. *h*-BN.** The *h*-BN crystal, like graphite, has a hexagonal structure, but with adjacent layers lying on top of each other, i.e., the B (N) atoms of one layer are positioned above N (B) atoms of the layer directly underneath. The experimental lattice parameters of the crystal are *a* = 2.503 and *c* = 6.661 Å.<sup>65</sup> The PBE functional fails to give a net attraction between the layers,

**Table 8. Lattice Parameters and Bulk Moduli of Layered Materials**

|                             | graphite             | <i>h</i> -BN       | V <sub>2</sub> O <sub>5</sub> |
|-----------------------------|----------------------|--------------------|-------------------------------|
| <i>a</i> (Å)                |                      |                    |                               |
| exptl                       | 2.462 <sup>a</sup>   | 2.503 <sup>b</sup> | 11.512 <sup>c</sup>           |
| PBE <sup>d</sup>            | 2.47                 | no binding         | 11.54                         |
| PBE-D2 <sup>d</sup>         | 2.46                 | 2.51               | 11.64                         |
| PBE-TS                      | 2.46                 | 2.51               | 11.68                         |
| vdW-DF1 <sup>e</sup>        | 2.47                 | 2.51               |                               |
| GGA+vdW <sup>f</sup>        |                      | 2.50               |                               |
| <i>c</i> (Å)                |                      |                    |                               |
| exptl                       | 6.707 <sup>a</sup>   | 6.661 <sup>b</sup> | 4.368 <sup>c</sup>            |
| PBE <sup>d</sup>            | 8.84                 | no binding         | 4.83                          |
| PBE-D2 <sup>d</sup>         | 6.45                 | 6.17               | 4.47                          |
| PBE-TS                      | 6.65                 | 6.71               | 4.35                          |
| vdW-DF1 <sup>e</sup>        | 7.52                 | 7.26               |                               |
| vdW-DF2 <sup>g</sup>        | 6.96                 |                    |                               |
| RPA                         | 6.68 <sup>h</sup>    | 6.61 <sup>i</sup>  |                               |
| GGA+vdW <sup>f</sup>        |                      | 6.55               |                               |
| <i>B</i> <sub>0</sub> (GPa) |                      |                    |                               |
| exptl                       | 34–42 <sup>a,j</sup> | 37 <sup>k</sup>    | 50 <sup>l</sup>               |
| PBE <sup>d</sup>            | 1                    | no binding         | 10                            |
| PBE-D2 <sup>d</sup>         | 38                   | 56                 | 33                            |
| PBE-TS                      | 56                   | 37                 | 38                            |
| vdW-DF1 <sup>e</sup>        | 12                   | 11                 |                               |
| GGA+vdW <sup>f</sup>        |                      | 43                 |                               |

<sup>a</sup>ref 60. <sup>b</sup>ref 65. <sup>c</sup>ref 68. <sup>d</sup>ref 19. <sup>e</sup>ref 62. <sup>f</sup>ref 30. <sup>g</sup>ref 63. <sup>h</sup>ref 64. <sup>i</sup>ref 67. <sup>j</sup>ref 61. <sup>k</sup>ref 81. <sup>l</sup>ref 82.

and as a result, the *c* lattice constant and the bulk modulus cannot be calculated with this method. The PBE-D2 method gives a value of the *c* lattice constant of 6.17 Å, about 0.5 Å smaller than the experimental value, while the PBE-TS method gives a value of 6.712 Å, only slightly larger than the experimental value. The PBE-D2 and PBE-TS procedures give values of 56 and 37 GPa, respectively, for the bulk modulus, as compared to the experimental value of 37 GPa.

*h*-BN has been investigated previously using the PBE-TS method, as implemented in the FHI-aims code. In this study, Marom et al.<sup>66</sup> showed that the electrostatic interactions, as captured using standard density functional methods, determine the optimal stacking mode and registry matching between the layers, while the dispersion interactions are important in fixing the interlayer distance. The resulting value of the *c* lattice parameter (6.66 Å) is about 0.05 Å smaller than that obtained in the present study using the same method implemented in VASP. The small difference in the two values of the lattice constant could be due to our use of pseudopotentials, while the calculations of Marom et al. were all electron. It could also arise from differences between the basis sets used in the two studies. GGA+vdW<sup>30</sup> calculations give *c* = 6.550 Å and *B*<sub>0</sub> = 43 GPa, which are also in good agreement with experimental values. As for graphite, the vdW-DF1 method fares poorly (*c* = 7.26 Å, *B*<sub>0</sub> = 11 GPa)<sup>62</sup> for BN. In contrast, the RPA/ACFDT method gives a value of *c* = 6.61 Å,<sup>67</sup> in excellent agreement with the experimental value.

**3.3.3. Vanadium Pentoxide (V<sub>2</sub>O<sub>5</sub>).** Vanadium is widely used in heterogeneous oxide catalysis. The V<sub>2</sub>O<sub>5</sub> crystal has a layered structure with an orthorhombic lattice with two formula units per unit cell with three structurally different oxygen atoms in each layer. The experimental values of the lattice constants are *a* = 11.51, *b* = 3.56, and *c* = 4.37 Å.<sup>68</sup> Bonding is covalent

within the layers, with *a* and *b* characterizing the intralayer spacings and the *c* lattice constant defining the interlayer spacing. As expected, the calculated *a* and *b* lattice parameters are relatively insensitive to the inclusion of dispersion corrections. The *c* lattice parameter is overestimated by 0.46 Å with the PBE functional. Both the PBE-D2 and PBE-TS give values of the *c* lattice parameter in good agreement with the experimental value. The PBE-D2 and PBE-TS methods yield bulk modulus values of 33 and 37 GPa, respectively, much closer to the experimental value of 50 GPa<sup>60</sup> than the result obtained from the PBE calculations (10 GPa).

#### 4. COVALENT SOLIDS

We also tested the PBE-TS and PBE-D2 methods on diamond and crystalline silicon, and the results are reported in Table 9.

**Table 9. Lattice Parameters and Bulk Moduli of Diamond and Crystalline Silicon**

|                     | diamond                     | Si    |
|---------------------|-----------------------------|-------|
|                     | <i>a</i> (Å)                |       |
| exptl <sup>a</sup>  | 3.543                       | 5.416 |
| PBE <sup>b</sup>    | 3.57                        | 5.47  |
| PBE-D2 <sup>b</sup> | 3.56                        | 5.41  |
| PBE-TS              | 3.55                        | 5.45  |
|                     | <i>B</i> <sub>0</sub> (GPa) |       |
| exptl <sup>a</sup>  | 443                         | 99.2  |
| PBE <sup>b</sup>    | 434                         | 89    |
| PBE-D2 <sup>b</sup> | 441                         | 98    |
| PBE-TS              | 446                         | 91    |

<sup>a</sup>Taken from ref 69 where zero-point and finite temperature corrections have been made to the experimental values. <sup>b</sup>ref 19.

For these two systems, calculations with the PBE functional without dispersion corrections already give values of the lattice constants and bulk modulus in good agreement with experimental values. However, the inclusion of dispersion corrections by means of either the PBE-D2 or the PBE-TS methods improves the agreement of the calculated lattice constants and bulk moduli with experimental results corrected for zero-point anharmonic effects and finite temperature effects.<sup>69</sup>

#### 5. PBESOL

The PBESol functional generally gives lattice constants in closer agreement with experimental values than does the PBE functional,<sup>21</sup> leading naturally to the question of whether the vdW-TS correction when used in conjunction with the PBESol functional would prove even more successful than PBE-TS.

Figure 4 reports for the crystals considered in this study the errors in the lattice constants obtained using the PBE and PBESol functionals with and without the vdW-TS correction. The errors are reported relative to the values of the experimental lattice constants. Although the experimental values of the lattice constants include the effects of vibrational anharmonicity and many-body interactions, in general, the errors in the calculated lattice constants are greater in magnitude than the sum of these corrections, making it meaningful to compare with uncorrected experimental values of the lattice constants. (Obviously, the Ne crystal is an exception due to its large anharmonicity contribution.) As expected, without dispersion corrections, PBESol outperforms PBE.

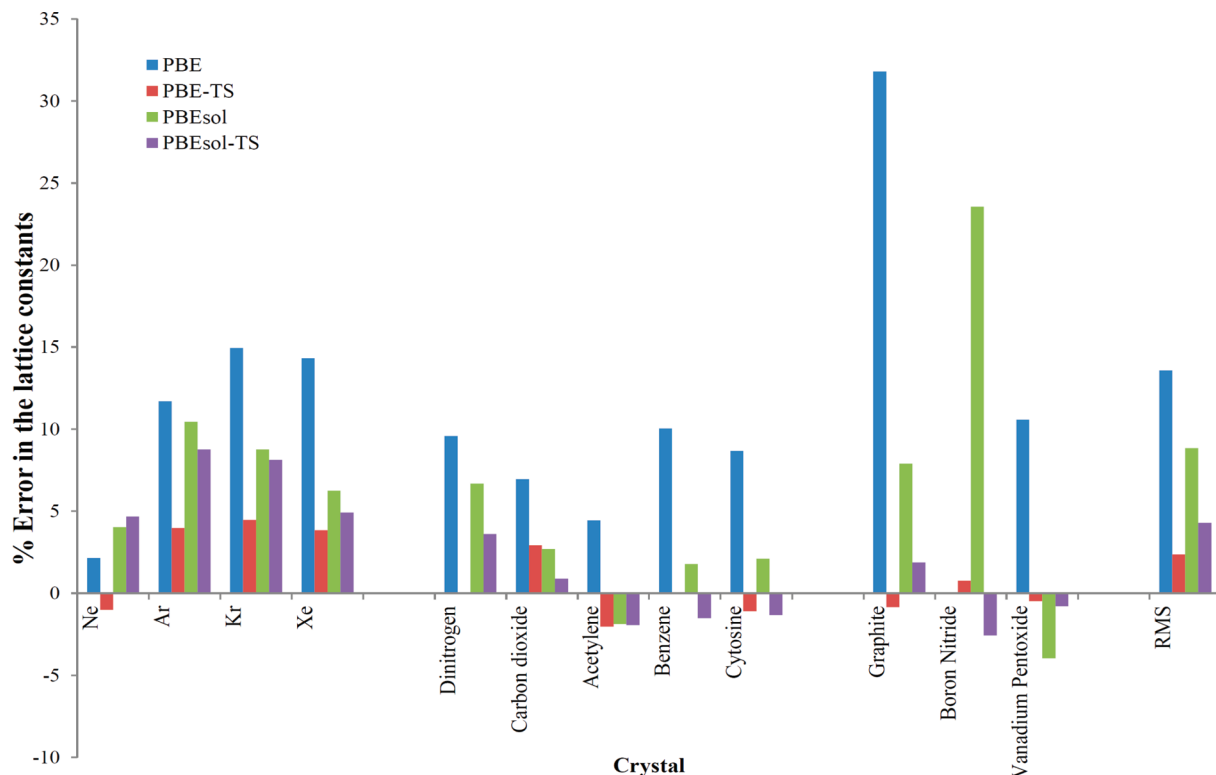


**Figure 4.** Errors in the calculated lattice constants for selected solids, using different theoretical methods. In case of molecular crystals, where the three lattice constants are not equal, the cube-root of the error in the volume is reported. In layered materials, the error in the *c* lattice constant is reported exclusively. (PBE does not bind BN; therefore no error is shown in the figure for this case.)

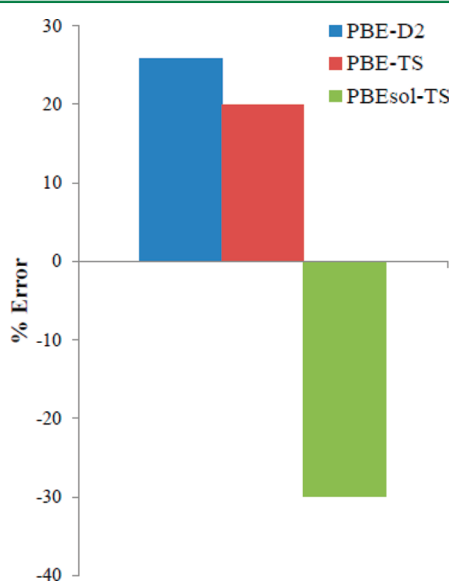
However, to our surprise, in general, PBEsol-TS does not perform better than PBE-TS in predicting the values of the lattice constants.

Figure 5 depicts the mean deviations of the calculated cohesive energies from the experimental values for the inert gas

As discussed in the text, all three of these contributions act so as to decrease the cohesive energy in magnitude. In other words, the 2-body contributions to the cohesive energies without ZPE effects should be larger in magnitude than the experimental values. As argued earlier in the text, it is these 2-body contributions to which comparison of the theoretical methods considered here is most meaningful. From Figure 5, it is seen that the mean values of the cohesive energies from the PBE-D2 and PBE-TS methods are, respectively, about 25 and 20% larger in magnitude than the experimental values. In contrast, the cohesive energies from the PBEsol-TS procedure are about 30% smaller in magnitude than the experimental values. In light of the above discussion, it is seen that the PBEsol-TS procedure is faring more poorly at describing the 2-body contributions to the cohesive energies than are the PBE-D2 or PBE-TS methods.

## 6. CONCLUSIONS

The vdW-TS scheme has been implemented in the VASP code and has been tested by calculating the lattice constants, cohesive energies, and bulk moduli of several solids. Overall, the vdW-TS approach when combined with the PBE functional performs much better than the PBE functional in the absence of dispersion corrections. For some systems and properties, the PBE-TS procedure gives better agreement with experimental results than the PBE-D2 procedure, but in other cases the PBE-D2 method gives properties in closer agreement with experimental results. In the present study, the vdW-TS method was employed with a noniterative Hirshfeld partitioning to determine the  $C_6$  coefficients for the interatomic dispersion corrections. We anticipate that the agreement of the calculated properties with experimental results would be improved by



**Figure 5.** The mean relative error in the PBE-D2, PBE-TS, and PBEsol-TS values of the cohesive energies.

and molecular crystal systems considered. The experimental numbers used in this comparison include many-body, vibrational ZPE, and, in some cases, finite temperature contributions.

adopting instead the iterative Hirshfeld<sup>70</sup> method, which was recently implemented in FHI-AIMS. Further improvement could be gained by adding  $C_8R^{-8}$  contributions and by including explicit contributions due to long-range 3-body dispersion contributions.

## AUTHOR INFORMATION

### Corresponding Author

\*E-mail: alsaidi@pitt.edu; jordan@pitt.edu.

### Notes

The authors declare no competing financial interest.

## ACKNOWLEDGMENTS

This research was supported by National Science Foundation, grant CHE 0809457. The calculations were carried out on computers in the University of Pittsburgh's Center for Molecular and Materials Simulations.

## REFERENCES

- (1) Payne, M. C.; Teter, M. P.; Allan, D. C.; Arias, T. A.; Joannopoulos, J. D. *Rev. Mod. Phys.* **1992**, *64*, 1045.
- (2) Kristyán, S.; Pulay, P. *Chem. Phys. Lett.* **1994**, *229*, 175.
- (3) Grimme, S. *J. Comput. Chem.* **2006**, *27*, 1787.
- (4) Grimme, S.; Antony, J.; Ehrlich, S.; Krieg, H. *J. Chem. Phys.* **2010**, *132*, 154104.
- (5) Rubeš, M.; Bludský, O.; Nachtigall, P. *ChemPhysChem* **2008**, *9*, 1702.
- (6) Rubeš, M.; Nachtigall, P.; Vondrášek, J.; Bludský, O. *J. Phys. Chem. C* **2009**, *113*, 8412.
- (7) Liu, Y.; Goddard, W. A. *J. Phys. Chem. Lett.* **2010**, *1*, 2550.
- (8) Tkatchenko, A.; Scheffler, M. *Phys. Rev. Lett.* **2009**, *102*, 073005.
- (9) Lilienfeld, O. A. v.; Tkatchenko, A. *J. Chem. Phys.* **2010**, *132*, 234109.
- (10) Hirshfeld, F. L. *Theo. Chem. Acct.: Theo., Comp., Model.* **1977**, *44*, 129.
- (11) Becke, A. D.; Johnson, E. R. *J. Chem. Phys.* **2005**, *122*, 154104.
- (12) Johnson, E. R.; Becke, A. D. *J. Chem. Phys.* **2006**, *124*, 174104.
- (13) Raghavachari, K.; Trucks, G. W.; Pople, J. A.; Head-Gordon, M. *Chem. Phys. Lett.* **1989**, *157*, 479.
- (14) Takatani, T.; Hohenstein, E. G.; Malagoli, M.; Marshall, M. S.; Sherrill, C. D. *J. Chem. Phys.* **2010**, *132*, 144104.
- (15) Jurecka, P.; Sponer, J.; Černý, J.; Hobza, P. *Phys. Chem. Chem. Phys.* **2006**, *8*.
- (16) Kresse, G.; Hafner, J. *Phys. Rev. B* **1993**, *47*, 558.
- (17) Kresse, G.; Furthmüller, J. *Phys. Rev. B* **1996**, *54*, 11169.
- (18) Perdew, J. P.; Burke, K.; Ernzerhof, M. *Phys. Rev. Lett.* **1996**, *77*, 3865.
- (19) Bučko, T.; Hafner, J.; Lebègue, S.; Ángyán, J. G. *J. Phys. Chem. A* **2010**, *114*, 11814.
- (20) Blum, V.; Gehrke, R.; Hanke, F.; Havu, P.; Havu, V.; Ren, X.; Reuter, K.; Scheffler, M. *Comput. Phys. Commun.* **2009**, *180*, 2175.
- (21) Perdew, J. P.; Ruzsinszky, A.; Csonka, G. I.; Vydrov, O. A.; Scuseria, G. E.; Constantin, L. A.; Zhou, X.; Burke, K. *Phys. Rev. Lett.* **2008**, *100*, 136406.
- (22) Blöchl, P. E. *Phys. Rev. B* **1994**, *50*, 17953.
- (23) Kresse, G.; Joubert, D. *Phys. Rev. B* **1999**, *59*, 1758.
- (24) Chen, Z.-M.; Çağin, T.; Goddard, W. A. *J. Comput. Chem.* **1997**, *18*, 1365.
- (25) Kerber, T.; Sierka, M.; Sauer, J. *J. Comput. Chem.* **2008**, *29*, 2088.
- (26) Brinck, T.; Murray, J. S.; Politzer, P. *J. Chem. Phys.* **1993**, *98*, 4305.
- (27) Chu, X.; Dalgarno, A. *J. Chem. Phys.* **2004**, *121*, 4083.
- (28) Bondi, A. *J. Phys. Chem.* **1964**, *68*, 441.
- (29) Harl, J.; Kresse, G. *Phys. Rev. B* **2008**, *77*, 045136.
- (30) Ortmann, F.; Bechstedt, F.; Schmidt, W. G. *Phys. Rev. B* **2006**, *73*, 205101.
- (31) Schwalbe, L. A.; Crawford, R. K.; Chen, H. H.; Aziz, R. A. *J. Chem. Phys.* **1977**, *66*, 4493.
- (32) McConvile, G. T. *J. Chem. Phys.* **1974**, *60*, 4093.
- (33) Lurie, N. A.; Shirane, G.; Skalyo, J. *Phys. Rev. B* **1974**, *9*, 2661.
- (34) Skalyo, J.; Endoh, Y.; Shirane, G. *Phys. Rev. B* **1974**, *9*, 1797.
- (35) Batchelder, D. N.; Losee, D. L.; Simmons, R. O. *Phys. Rev.* **1967**, *162*, 767.
- (36) Peterson, O. G.; Batchelder, D. N.; Simmons, R. O. *Phys. Rev.* **1966**, *150*, 703.
- (37) Losee, D. L.; Simmons, R. O. *Phys. Rev.* **1968**, *172*, 944.
- (38) Sears, D. R.; Klug, H. P. *J. Chem. Phys.* **1962**, *37*, 3002.
- (39) Langreth, D. C.; Perdew, J. P. *Solid State Commun.* **1975**, *17*, 1425.
- (40) Andersson, Y.; Langreth, D. C.; Lundqvist, B. I. *Phys. Rev. Lett.* **1996**, *76*, 102.
- (41) Rościszewski, K.; Paulus, B.; Fulde, P.; Stoll, H. *Phys. Rev. B* **2000**, *62*, 5482.
- (42) Beate, P. *Phys. Rep.* **2006**, *428*, 1.
- (43) Rościszewski, K.; Paulus, B.; Fulde, P.; Stoll, H. *Phys. Rev. B* **1999**, *60*, 7905.
- (44) Ogilvie, J. F.; Wang, F. Y. H. *J. Mol. Struct.* **1992**, *273*, 277.
- (45) Kumar, A.; Meath, W. *Mol. Phys.* **1985**, *54*, 823.
- (46) Wang, F.-F.; Jenness, G.; Al-Saidi, W. A.; Jordan, K. D. *J. Chem. Phys.* **2010**, *132*, 134303.
- (47) Patton, D. C.; Pederson, M. R. *Phys. Rev. A* **1997**, *56*, R2495.
- (48) Dobson, J. F.; McLennan, K.; Rubio, A.; Wang, J.; Gould, T.; Le, H. M.; Dinte, B. P. *Aust. J. Chem.* **2001**, *54*, 513.
- (49) Wen, S.; Beran, G. J. O. *J. Chem. Theory Comput.* **2011**, *7*, 3733.
- (50) Chickos, J. S.; William E. Acree, J. *J. Phys. Chem. Ref. Data* **2002**, *31*, 537.
- (51) LeSar, R.; Gordon, R. G. *J. Chem. Phys.* **1983**, *78*, 4991.
- (52) Schuch, A. F.; Mills, R. L. *J. Chem. Phys.* **1970**, *52*, 6000.
- (53) Kuan, T.-S.; Warshel, A.; Schnepf, O. *J. Chem. Phys.* **1970**, *52*, 3012.
- (54) Kybett, B. D.; Carroll, S.; Natalis, P.; Bonnell, D. W.; Margrave, J. L.; Franklin, J. L. *J. Am. Chem. Soc.* **1966**, *88*, 626.
- (55) Berland, K.; Hyldgaard, P. *J. Chem. Phys.* **2010**, *132*, 134705.
- (56) David, W. I. F.; Ibbserson, R. M.; Jeffrey, G. A.; Ruble, J. R. *Physica B* **1992**, *180–181* (Part 2), 597.
- (57) Lu, D.; Li, Y.; Rocca, D.; Galli, G. *Phys. Rev. Lett.* **2009**, *102*, 206411.
- (58) Podeszwa, R.; Rice, B. M.; Szalewicz, K. *Phys. Rev. Lett.* **2008**, *101*, 115503.
- (59) Fedorov, I. A.; Zhuravlev, Y. N.; Berveno, V. P. *Phys. Chem. Chem. Phys.* **2011**, *13*, 5679.
- (60) Zhao, Y. X.; Spain, I. L. *Phys. Rev. B* **1989**, *40*, 993.
- (61) Hanfland, M.; Beister, H.; Syassen, K. *Phys. Rev. B* **1989**, *39*, 12598.
- (62) Rydberg, H.; Dion, M.; Jacobson, N.; Schröder, E.; Hyldgaard, P.; Simak, S. I.; Langreth, D. C.; Lundqvist, B. I. *Phys. Rev. Lett.* **2003**, *91*, 126402.
- (63) Berland, K.; Borck, Ø.; Hyldgaard, P. *Comput. Phys. Commun.* **2011**, *182*, 1800.
- (64) Lebègue, S.; Harl, J.; Gould, T.; Ángyán, J. G.; Kresse, G.; Dobson, J. F. *Phys. Rev. Lett.* **2010**, *105*, 196401.
- (65) Pease, R. *Acta Crystallogr.* **1952**, *5*, 356.
- (66) Marom, N.; Bernstein, J.; Garel, J.; Tkatchenko, A.; Joselevich, E.; Kronik, L.; Hod, O. *Phys. Rev. Lett.* **2010**, *105*, 046801.
- (67) Marini, A.; García-González, P.; Rubio, A. *Phys. Rev. Lett.* **2006**, *96*, 136404.
- (68) Enjalbert, R.; Galy, J. *Acta Crystallogr.* **1986**, *42*, 1467.
- (69) Csonka, G. I.; Perdew, J. P.; Ruzsinszky, A.; Philipsen, P. H. T.; Lebègue, S.; Paier, J.; Vydrov, O. A.; Ángyán, J. G. *Phys. Rev. B* **2009**, *79*, 155107.
- (70) Bultinck, P.; Van Alsenoy, C.; Ayers, P. W.; Carbó-Dorca, R. *J. Chem. Phys.* **2007**, *126*.
- (71) Simon, A.; Peters, K. *Acta Crystallogr.* **1980**, *36*, 2750.
- (72) McMullan, R. K.; Kvick, A.; Popelier, P. *Acta Crystallogr.* **1992**, *48*, 726.

- (73) Yoo, C. S.; Kohlmann, H.; Cynn, H.; Nicol, M. F.; Iota, V.; LeBihan, T. *Phys. Rev. B* **2002**, *65*, 104103.
- (74) Yildirim, T.; Gehring, P. M.; Neumann, D. A.; Eaton, P. E.; Emrick, T. *Phys. Rev. Lett.* **1997**, *78*, 4938.
- (75) Natkaniec, I.; Belushkin, A. V.; Dyck, W.; Fuess, H.; Zeyen, C. M. E. Z. *Kristallogr.* **1983**, *163*, 285.
- (76) Mason, R. *Acta Crystallogr.* **1964**, *17*, 547.
- (77) Meijer, E. J.; Sprik, M. *J. Chem. Phys.* **1996**, *105*, 8684.
- (78) Vaidya, S. N.; Kennedy, G. C. *J. Chem. Phys.* **1971**, *55*, 987.
- (79) Barker, D. L.; Marsh, R. E. *Acta Crystallogr.* **1964**, *17*, 1581.
- (80) Burkinshaw, P. M.; Mortimer, C. T. *J. Chem. Soc., Dalton Trans.* **1984**, *75*.
- (81) Solozhenko, V. L.; Will, G.; Elf, F. *Solid State Commun.* **1995**, *96*, 1.
- (82) Loa, I.; Grzechnik, A.; Schwarz, U.; Syassen, K.; Hanfland, M.; Kremer, R. K. *J. Alloys Compd.* **2001**, *317–318*, 103.